Snake venom disintegrins: novel dimeric disintegrins and structural diversification by disulphide bond engineering

Juan J. CALVETE*[1], M. Paz MORENO-MURCIANO*, R. David G. THEAKSTON†, Dariusz G. KISIEL‡ and Cezary MARCINKIEWICZ‡

*Instituto de Biomedicina de Valencia, Consejo Superior de Investigaciones Cientificas, Jaime Roig 11, 46010 Valencia, Spain, †Alistair Reid Venom Research Unit, Liverpool School of Tropical Medicine, Pembroke Place, Liverpool L3 5QA, U.K., and ‡Biotechnology Center, Temple University College of Science and Technology, 1900 N. 12th Street, Philadelphia, PA 19122-6078, U.S.A.

We report the isolation and amino acid sequences of six novel dimeric disintegrins from the venoms of *Vipera lebetina obtusa* (VLO), *V. berus* (VB), *V. ammodytes* (VA), *Echis ocellatus* (EO) and *Echis multisquamatus* (EMS). Disintegrins VLO4, VB7, VA6 and EO4 displayed the RGD motif and inhibited the adhesion of K562 cells, expressing the integrin $\alpha5\beta1$ to immobilized fibronectin. A second group of dimeric disintegrins (VLO5 and EO5) had MLD and VGD motifs in their subunits and blocked the adhesion of the $\alpha4\beta1$ integrin to vascular cell adhesion molecule 1 with high selectivity. On the other hand, disintegrin EMS11 inhibited both $\alpha5\beta1$ and $\alpha4\beta1$ integrins with almost the same degree of specificity. Comparison of the amino acid sequences of the dimeric disintegrins with those of other disintegrins by multiple-sequence alignment and phylogenetic analysis, in conjunction with current biochemical and genetic data, supports the view that the different disintegrin subfamilies evolved from a common ADAM (a disintegrin and metalloproteinase-like) scaffold and that structural diversification occurred through disulphide bond engineering.

Key words: disintegrin, disulphide bond, evolution, protein sequence, snake venom protein.

INTRODUCTION

Crotalid and viperid venoms contain a large number of haemorrhagic proteins. Haemorrhage is the result of the synergistic action of certain metalloproteinases which degrade the extracellular matrix surrounding blood vessels and proteins that interfere with haemostasis (reviewed in [1]). Snake venom haemorrhagic metalloproteinases have been classified according to their domain structure into three classes [2]. PI metalloproteinases (20–30 kDa) are single-domain proteins with relatively weak haemorrhagic activity. The PII class metalloproteinases (30–60 kDa) contain a disintegrin domain at the C-terminus of a metalloproteinase domain structurally similar to that in the PI class. Haemorrhagins of the PIII class are large toxins (60–100 kDa) with the most potent activity, and comprise multidomain enzymes built up of an N-terminal metalloproteinase domain and C-terminal disintegrin-like and cysteine-rich domains [1–3]. Disintegrins are released in the venoms by proteolytic processing of PII metalloproteinases [2,3], and inhibit integrin–ligand interactions. However, the involvement of the disintegrin-like domains of PIII haemorrhagins in integrin recognition remains controversial [4].

Disintegrins are divided into five different groups according to their polypeptide length and number of disulphide bonds [4–7]. The first group includes short-sized disintegrins, including echistatin, eristocophin, eristostatin and ocellatusin, which are composed of 49–51 residues and four disulphide bonds [8–10]. The second group is formed by medium-sized disintegrins, which contain approx. 70 amino acids and six disulphide bonds [8,11–13]; most of the 50 or more different disintegrins characterized to date, including trigramin, kistrin, flavoridin, albolabrin and barbourin, belong to this group. The third group includes the long-sized disintegrin bitistatin, an 84-residue polypeptide cross-linked by seven disulphide bonds [14] and salmosin 3 [15]. The disintegrin domains of PIII snake-venom metalloproteinases containing approx. 100 amino acids with 16 cysteine residues involved in the formation of eight disulphide bonds [1–4,16] constitute the fourth group of the disintegrin family. Unlike short-, medium- and long-sized disintegrins, which are single-chain molecules [4], the fifth group is composed of homo- and heterodimers. Dimeric disintegrins like contortrostatin, EC3 and EMF-10 [5–7] contain subunits of approx. 67 residues with ten cysteine residues involved in the formation of four intrachain disulphide bonds and two interchain cystine linkages [17]. Bilitoxin-1 represents another homodimeric disintegrin comprising disulphide-bonded polypeptides each containing 15 cysteine residues [18].

The integrin-inhibitory activity of disintegrins depends on the appropriate pairing of cysteine residues, which determine the conformation of the inhibitory loop. In most single-chain disintegrins, the active sequence is the tripeptide RGD [4], the exceptions being barbourin and ussuristatin 2, two medium-sized disintegrins possessing an active KGD sequence [19,20] and atrolysin E, which has an MVD motif in its inhibitory loop [3]. NMR studies of several short- (echistatin) and medium-sized (kistrin, flavoridin, albolabrin) disintegrins revealed that the active tripeptide is located at the apex of a mobile loop protruding 14–17 Å (1 Å = 0.1 nm) from the protein core [11,21–23]. RGD-containing disintegrins show different levels of binding affinity and selectivity towards integrins which recognize the RGD sequence in their ligands (i.e. αIIb$\beta3$, $\alpha v\beta3$ and $\alpha5\beta1$ [24]). KGD-containing barbourin inhibits the αIIb$\beta3$ integrin with a

Abbreviations used: ADAM, a disintegrin and metalloproteinase-like; CHO, Chinese-hamster ovary; EMS, disintegrin from the venom of *Echis multisquamatus*; EO, VA, VB, VLO, disintegrins from the venoms of *Echis ocellatus*, *Vipera ammodytes*, *V. berus* and *V. lebetina obtusa* respectively; HBSS, Hanks balanced salt solution; MALDI–TOF-MS; matrix-assisted laser-desorption ionization–time-of-flight mass spectrometry; PE, pyridylethylated; TFA, trifluoroacetic acid; VCAM, vascular cell adhesion molecule.

[1] To whom correspondence should be addressed (e-mail jcalvete@ibv.csic.es).

high degree of selectivity [19]. The integrin specificity profile of atrolysin E is unknown, although due to its inhibition of ADP- and collagen-stimulated platelet aggregation, αIIbβ3 may be one of its target receptor(s) [25].

Dimeric disintegrins exhibit the highest level of sequence diversity in their integrin-binding motifs. EC3, a heterodimeric disintegrin from *Echis carinatus* (=*E.c. sochureki* or *E. sochureki*) venom, is a selective and potent antagonist of the binding of $\alpha4\beta1$ and $\alpha4\beta7$ integrins to immobilized vascular cell adhesion molecule (VCAM)-1 and mucosal addressin cell adhesion molecule (MAdCAM)-1 respectively. It is also a weaker inhibitor of $\alpha5\beta1$ and αIIbβ3 integrins and does not inhibit αvβ3 integrin [6]. The inhibitory activity of EC3 towards $\alpha4$ integrins is associated with the MLD sequence of its B subunit. The A subunit of EC3 contains a VGD motif, and the ability of EC3 to inhibit $\alpha5\beta1$ resides in both subunits [6]. EMF-10, another heterodimeric disintegrin isolated from the venom of *Eristocophis macmahoni*, is an extremely potent and selective inhibitor of integrin $\alpha5\beta1$, binding to fibronectin and partially inhibiting the adhesion of cells expressing integrins αIIbβ3, αvβ3 and $\alpha4\beta1$ to their appropriate ligands [7]. Selective recognition of $\alpha5\beta1$ by EMF-10 is associated with the MGD(W) sequence, a motif located in the active loop of the B subunit, and expression of $\alpha5\beta1$-inhibitory activity may also depend on the RGD(N) motif in the A subunit [7]. The presence of a WGD motif in CC8, a heterodimeric disintegrin isolated from the venom of the North African sand viper, *Cerastes cerastes cerastes*, has been reported to increase its inhibitory effect on αIIbβ3, αvβ3 and $\alpha5\beta1$ integrins [26]. Dimeric disintegrins are thus valuable tools for identifying novel integrin-binding sequence motifs, which may shed light on the structural requirements of selective integrin inhibition.

We have determined the amino acid sequences of seven novel dimeric disintegrin subunits isolated from the venoms of *Vipera lebetina obtusa*, *V. berus*, *V. ammodytes*, *E. ocellatus* and *E. multisquamatus*. Their integrin-inhibition selectivity was investigated using a panel of cell lines expressing defined integrin receptors. The apparent common ancestry of mammalian metalloproteinases and snake venom haemorrhagins, from which the disintegrin domains evolved after mammals and reptiles diverged [27], prompted us to investigate possible evolutionary pathways giving rise to the large structural diversity within different groups of the disintegrin family.

METHODS

Purification of dimeric disintegrins

Freeze-dried venoms from *V.l. obtusa*, *V. berus*, *E. ocellatus* and *E. multisquamatus*, purchased from Latoxan Serpentarium (Rosans, France) and *V. ammodytes* (Sigma), were dissolved in 0.1 % trifluoroacetic acid (TFA) at a concentration of approx. 30 mg/ml. Insoluble material was discarded after centrifugation at 5000 rev./min for 5 min and the clear supernatant was fractionated by reverse-phase HPLC on a Vydac C-18 (250 mm × 10 mm) column (Vydac, Hesperia, CA, U.S.A.), eluting at 2 ml/min with a linear gradient of 0.1 % TFA in water (solution A) and 0.1 % TFA in acetonitrile (solution B). Chromatographic conditions were 0–80 % B over 45 min. Separations were monitored at 220 nm, and fractions were collected manually and dried using a Speed-Vac system. HPLC-separated fractions were dissolved in water and tested for their ability to inhibit the adhesion of cultured cells (see below). Active HPLC fractions were rechromatographed using the same HPLC system but the column was developed with a flatter gradient (0–60 % B over 45 min). HPLC peaks displaying cell adhesion inhibition activity were freeze-dried. Protein purity was tested by SDS/PAGE and matrix-assisted laser-desorption ionization–time-of-flight mass spectrometry (MALDI–TOF-MS), performed at the Wistar Mass Spectrometry Facility (Philadelphia, PA, U.S.A.) and the Instituto de Biomedicina de Valencia (Spain), using in both cases a PE-Biosystems Voyager-DE Pro instrument and 3,5-dimethoxy-4-hydroxycinnamic acid (sinapinic acid) saturated in 50 % acetonitrile and 0.1 % TFA as matrix. For quantification of free thiol groups and disulphide bonds, dimeric disintegrins [0.5 mg/ml in 100 mM ammonium bicarbonate (pH 8.3), containing 6 M guanidinium chloride] were incubated either with 10 mM iodoacetamide for 2 h at room temperature (24 °C) or with 1 % (v/v) 2-mercaptoethanol for 2 min at 100 °C, followed by the addition of a 10-fold molar excess of 4-vinylpyridine over a reducing agent and incubation for 1 h at room temperature. Samples were dialysed against deionized (MilliQ) water, freeze-dried, and were subjected to amino acid analysis (after sample hydrolysis with 6 M HCl for 24 h at 110 °C) using a Pharmacia AlphaPlus analyser, and MALDI–TOF-MS.

Cell adhesion inhibition assays

The following cell lines were employed: K562 cells transfected with the $\alpha1$, $\alpha2$ and $\alpha6$ subunits of integrins were provided by Dr M. Hemler (Dana Farber Cancer Institute, Boston, MA, U.S.A.); A5 cells and Chinese-hamster ovary (CHO) cells transfected with the αIIbβ3 integrin were provided by Dr M Ginsberg (Scripps Research Institute, La Jolla, CA, U.S.A.); K562 and Jurkat cells, which express integrins $\alpha5\beta1$ and $\alpha4\beta1$ respectively, were purchased from A.T.C.C. (Manassas, VA, U.S.A.). The inhibition of cells labelled with 5-chloromethyl fluorescein diacetate to ligands immobilized on a 96-well microtitre plate (Falcon, Pittsburg, PA, U.S.A.) was assayed as described previously [24]. Briefly, fibrinogen (provided by Dr A. Budzynski, Temple University, Philadelphia, PA, U.S.A.), fibronectin (Sigma), vitronectin (Chemicon, Ternecula, CA, U.S.A.), laminin (ICN Biomedicals, Irvine, CA, U.S.A.), VCAM-1 (provided by Dr P. Wainreb, Biogen Inc., Cambridge, MA, U.S.A.), collagen types I and IV (Chemicon) were immobilized on a 96-well microtitre plate (Falcon) in PBS (or in 0.02 M acetic acid for collagens) overnight at 4 °C. Wells were blocked with 1 % BSA in Hanks balanced salt solution (HBSS) containing 3 mM $CaCl_2$ and 3 mM $MgCl_2$. The cells were labelled with fluorescein by incubation at 37 °C for 15 min with 12.5 μM 5-chloromethyl fluorescein diacetate in HBSS containing calcium and magnesium (for collagen receptors, HBSS buffer containing 3 mM $MgCl_2$). Cells were freed from unbound ligand by washing with the same buffer. Labelled cells (1×10^5/sample) were added to the wells in the presence or absence of inhibitors and incubated at 37 °C for 30 min. Unbound cells were removed by aspiration, the wells were washed and bound cells were lysed by adding 0.5 % Triton X-100. In parallel, the standard curve was prepared in the same plate using known concentrations of labelled cells. The plates were read using a Cytofluor 2350 fluorescence plate reader (Millipore, Bedford, MA, U.S.A.) at an excitation wavelength of 485 nm using a 530 nm emission filter.

Isolation and structural characterization of pyridylethylated (PE) subunits

Dimeric disintegrins [0.5 mg/ml in 0.1 M Tris/HCl (pH 8.5), 4 mM EDTA, 6 M guanidinium chloride] were reduced with 3.2 mM dithiothreitol for 2 h at room temperature and in the dark. Reduced proteins were alkylated by the addition of a 2-fold molar excess of 4-vinylpyridine over a reducing reagent. PE subunits were isolated by reverse-phase HPLC on a C_{18} column

developed with a linear gradient of solution A and solution B, and were denoted 'A' or 'B' according to their elution order. The isolated PE subunits were initially characterized by N-terminal sequencing (using either an Applied Biosystems 477A or a Beckman Porton LF-3000 instrument following the manufacturer's instructions), amino acid analysis and MALDI–TOF-MS [as above but using α-cyano-4-hydroxycinnamic acid saturated in 50 % (v/v) acetonitrile and 0.1 % TFA as the matrix]. The primary structures of PE polypeptides were deduced from N-terminal sequence analysis of overlapping peptides obtained by proteolytic digestions with endoproteinases Lys-C [2 mg/ml protein in 100 mM ammonium bicarbonate (pH 8.3); Boehringer Mannheim] for 18 h at 37 °C using an enzyme/substrate ratio of 1:100 (w/w) and degradation with CNBr [10 mg/ml protein and 100 mg/ml CNBr in 70 % (v/v) formic acid for 6 h at room temperature, under N_2 atmosphere and in the dark]. Peptides were separated by reverse-phase HPLC using a 4 mm × 250 mm C_{18} (particle size = 5 μm) Lichrospher RP100 (Merck) column eluting at 1 ml/min with a linear gradient of solution A and solution B.

Disintegrin domain sequences

A non-redundant database of amino acid sequences of snake venom disintegrins was constructed from primary literature on disintegrins and by sequence homology searches in the SwissProt, TREMBL (http://www.expasy.ch) and GenBank® (http://www.ncbi.nlm.nih.gov) databases using the BLAST program [28] implemented in the WU-BLAST2 search engine at http://www.bork.embl-heidelberg.de. Sequence alignment was made by CLUSTALW program [29]. Databank accession numbers or primary references for all sequences are given in Figure 3. A list of the 233 disintegrin domain proteins from any organism is available in the PFAM protein families' database addressing http://www.sanger.ac.uk/cgi-bin/Pfam/getallproteins.pl?name=disintegrin&acc=PF00200&verbose=true&type=full&zoom_factor=0.5&list=View+Graphic and in the SMART website (http://smart.embl-heidelberg.de/smart/get_members.pl?WHAT=NRDB_COUNT&NAME=DISIN). The amino acid sequences of mammalian ADAM (a disintegrin and metalloproteinase-like) proteins were retrieved from http://www.gene.ucl.ac.uk/nomenclature/genefamily/metallo.html.

Phylogenetic analysis

The package of programs PHYLIP (the PHYLogeny Inference Package; obtained at: http://evolution.genetics.washington.edu/phylip.html) [30] and MEGA (Molecular Evolutionary Genetic Analysis; http://www.megasoftware.net) [31] were employed for inferring phylogenies (evolutionary trees) from a multiple alignment of disintegrin sequences. Methods that are available in the package include parsimony, distance matrix and likelihood methods, including bootstrapping and consensus trees.

RESULTS AND DISCUSSION

Characterization of novel dimeric disintegrins

The venom proteins of *E. ocellatus*, *E. multisquamatus*, *V.l. obtusa*, *V. berus* and *V. ammodytes* were separated by reverse-phase HPLC. The fractions were denoted by the initials of the snake species followed by the HPLC fraction number. Screening against a panel of integrins [24] identified seven proteins that were classified into three groups according to their main integrin-inhibition specificity (Table 1). The first group included disintegrins from the venoms of *E. ocellatus* (EO4), *V.l. obtusa* (VLO4), *V. berus* (VB7) and *V. ammodytes* (VA6). These disintegrins inhibited the adhesion of cells expressing the RGD-dependent integrin $\alpha5\beta1$ (K562) to immobilized fibronectin. The second group comprising EO5 and VLO5 blocked the adhesion of the $\alpha4\beta1$ integrin to VCAM-1. The third group included disintegrin from the venom of *E. multisquamatus* (EMS11), which inhibited the adhesion of both K562 and Jurkat cells to immobilized fibronectin and VCAM-1 respectively, with almost the same degree of specificity. The inhibitory activity of these seven disintegrins on the adhesion of A5 cells (CHO cells transfected with integrin αIIb$\beta3$) to fibrinogen was 50–100-fold lower than their main integrin-inhibitory activity. On the other hand, none of the disintegrins significantly inhibited the binding of K562 cells expressing integrins $\alpha1\beta1$, $\alpha2\beta1$ and $\alpha6\beta1$ to their respective immobilized ligands (Table 1).

The seven proteins were purified to homogeneity using the two-step reverse-phase HPLC method used in previous studies [6,7,26,32]. Figure 1 illustrates the steps along the purification protocol of native disintegrin VB7 and its PE subunits. The other disintegrins and their subunits were purified according to the same general scheme. SDS/PAGE showed that each of these proteins had apparent molecular masses of 14–15 kDa (non-reducing conditions) and 7 kDa (reduced samples), indicating that each of the seven proteins contained two disulphide-bonded subunits. Reverse-phase HPLC was used to separate the subunits after reduction and pyridylethylation of the native proteins, and the purified subunits were denoted PE-'A' or PE-'B' according to their elution order. Table 2

Table 1 Comparison of the inhibitory activities of dimeric disintegrins on the adhesion of different cell lines expressing defined integrins to immobilized ligands

The data represent the means for three experiments. Coll, collagen; LM, laminin; FN, fibronectin; FG, fibrinogen; α1-, α2- and α6-K562, K562 cells transfected with $\alpha1$, $\alpha2$ or $\alpha6$ integrin subunits respectively; A5, CHO cells transfected with αIIb$\beta3$ integrin.

			IC_{50} (nM)						
Cell line	Integrin receptor	Ligand	VB7	VLO5	EO5	EMS11	EO4	VLO4	VA6
α1-K562	$\alpha1\beta1$	Coll IV	> 10 000	> 10 000	> 10 000	> 10 000	> 10 000	> 10 000	> 10 000
α2-K562	$\alpha2\beta1$	Coll I	> 10 000	> 10 000	> 10 000	> 10 000	> 10 000	> 10 000	> 10 000
α6-K562	$\alpha6\beta1$	LM	> 10 000	> 10 000	> 10 000	> 10 000	> 10 000	> 10 000	> 10 000
K562	$\alpha5\beta1$	FN	1.1	3400	690	6.0	1.2	3.5	3.8
Jurkat	$\alpha4\beta1$	VCAM-1	4830	5.5	9.5	14	1850	1400	2450
A5	αIIb$\beta3$	FG	420	760	980	350	118	115	144

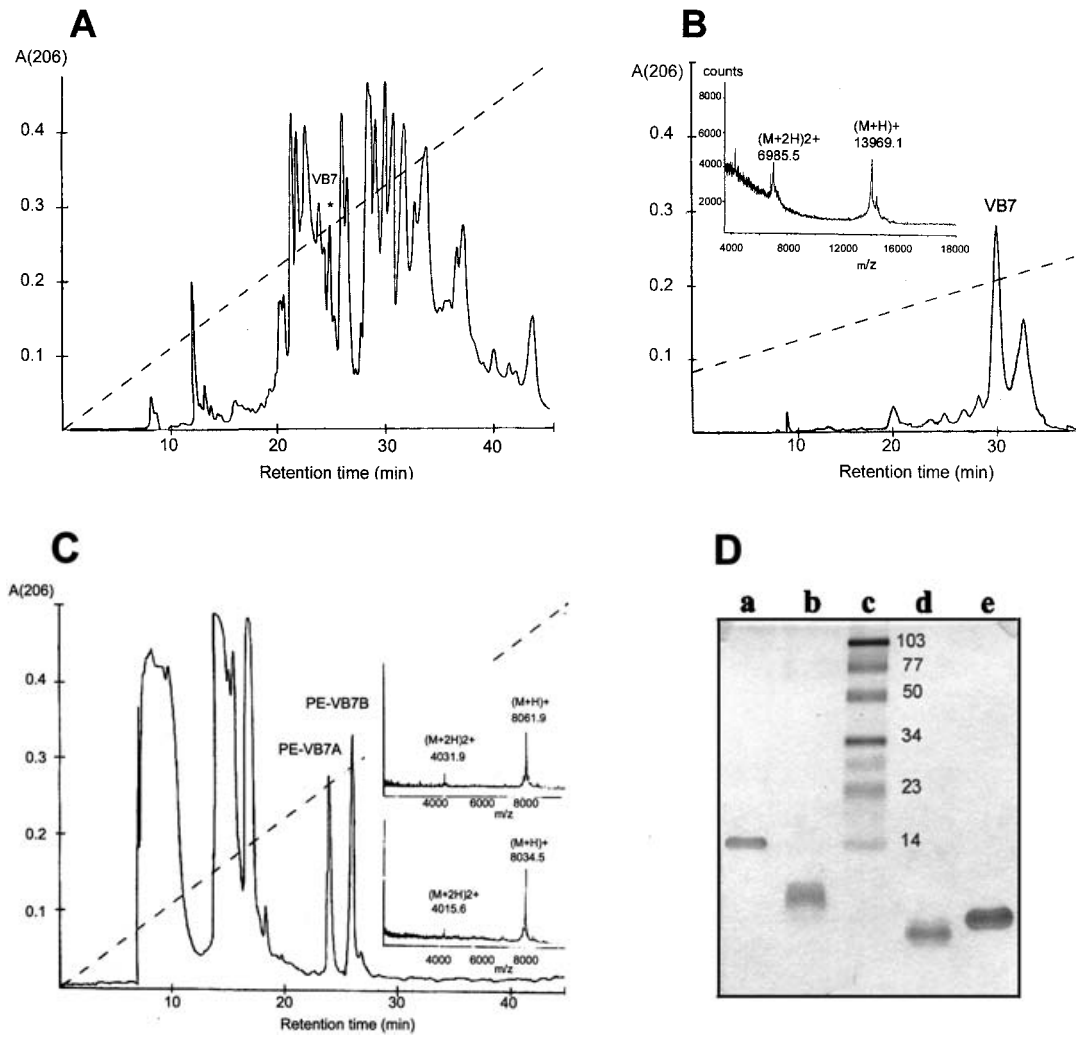

Figure 1 Purification of dimeric disintegrins

The procedure followed in the purification of disintegrin VB7 is illustrated.(**A**) Reverse-phase chromatographic separation (0–80 % B over 45 min) of the crude venom of *V. berus*. The elution position of purified VB7 is indicated by an asterisk. (**B**) Fraction VB7 from (**A**) was further purified using the same HPLC system as in (**A**) but developing the column with a flatter gradient (0–60 % B over 45 min). The inset shows a MALDI–TOF-MS analysis of purified VB7. (**C**) Reverse-phase HPLC separation of the PE subunits of VB7. The mass spectra of PE-VB7A and PE-VB7B are shown. (**D**) SDS/PAGE of non-reduced (lane a) and reduced (lane b) VB7, purified as in (**B**). Lanes d and e, PE-A and PE-B subunits of VB7 isolated as in (**C**). Lane c, molecular-mass markers (Bio-Rad, Hercules, CA, U.S.A.), from top to bottom: phosphorylase *b* (103 kDa), BSA (77 kDa), ovalbumin (50 kDa), carbonic anhydrase (34 kDa), soya-bean trypsin inhibitor (23 kDa) and lysozyme (14 kDa).

Table 2 Molecular features of native disintegrins and their subunits isolated from the venoms of *E. ocellatus* (EO), *E. multisquamatus* (EMS), *V.l. obtusa* (VLO), *V. berus* (VB) and *V. ammodytes* (VA)

	Molecular mass (kDa)				
		PE subunits		Integrin-binding motif	
Disintegrin	Native	A	B	A	B
EO4	14.526	8.416	8.196	RGD	VGD
EO5	14.515	8.456	8.196	MLD	VGD
EMS11	14.908	8.521	8.514	MLD	n.d.*
VLO4	14.196	8.163	8.163	RGD	RGD
VLO5	14.728	8.165	8.690	VGD	MLD
VB7	13.969	8.062	8.034	RGD	KGD
VA6	14.046	8.078	8.078	RGD	RGD

*n.d., not determined.

shows the molecular masses of the native proteins and their PE subunits from MALDI–TOF-MS. The molecular masses of the native proteins did not change on incubation with alkylating reagents in denaturing, non-reducing buffers, showing that EO4, EO5, EMS11, VLO4, VLO5, VB7 and VA6 did not contain free thiol groups. On the other hand, the mass difference of approx. 2.128 kDa between the sum of the PE subunits and the native proteins indicated that each disintegrin contained 20 cysteine residues involved in the formation of ten inter- and intrasubunit disulphide bonds. The amino acid sequences of EO4, EO5, EMS11, VLO4, VLO5, VB7 and VA6 subunits were established using automated Edman degradation of the reduced and PE protein and of peptides obtained after degradation of the PE subunits with endoproteinase Lys-C and CNBr (Figure 2). The polypeptides display a large amino acid sequence similarity between themselves and with the members of the subfamily of dimeric disintegrins (Figure 3), including the position of ten cysteine residues per subunit, which is a conserved feature of

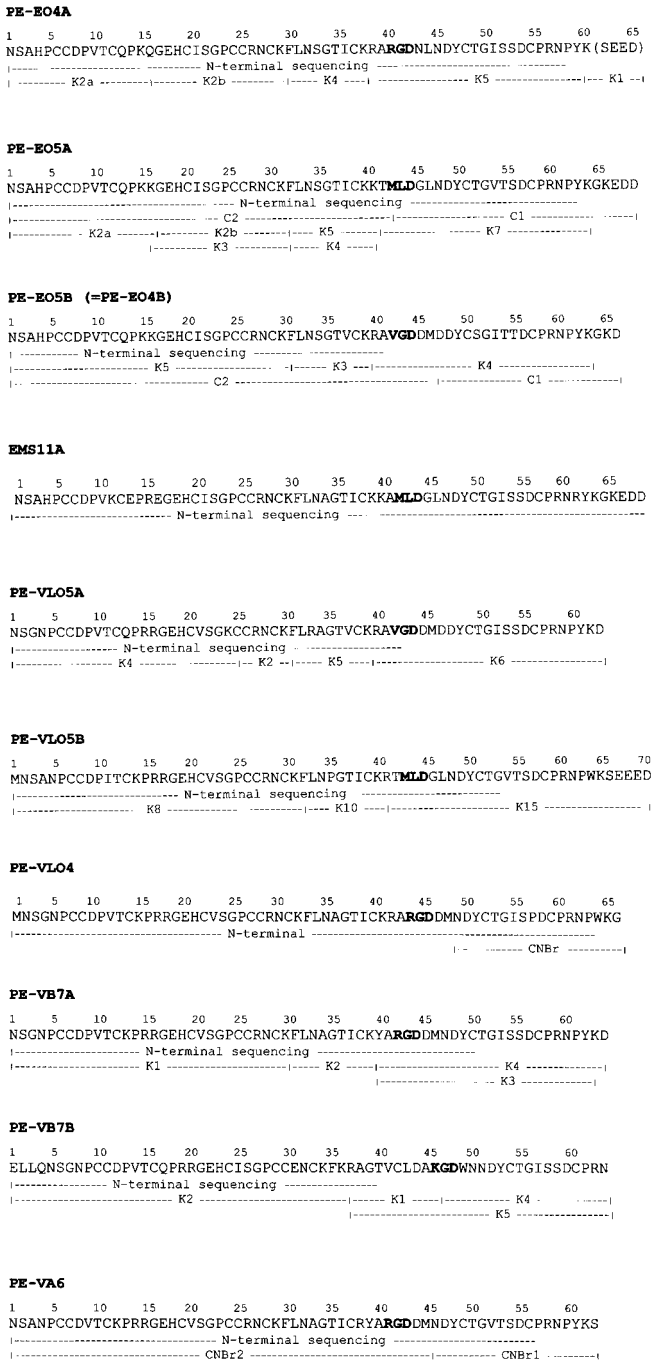

Figure 2 Amino acid sequences (one-letter code) of disintegrin subunits isolated from the venoms of *E. ocellatus* (EO), *V.l. obtusa* (VLO), *V. berus* (VB) and *V. ammodytes* (VA)

The sequences were established by automated Edman degradation of the PE proteins and of overlapping peptides isolated by reverse-phase HPLC after degradation of the PE proteins with endoproteinase Lys-C (K) and CNBr. VLO4 and VA6 are homodimers.

all polypeptides of this group. Except for VLO4 and VA6, which are homodimers, all the other proteins are heterodimers. EO4 and EO5, the two dimeric disintegrins isolated from the venom of *E. ocellatus*, share the B subunit (Table 2, Figure 2). Similarly, EC3 and EC6, two dimeric disintegrins from the venom of *E. carinatus* (=*E.c. sochureki* or *E. sochureki*) [6,32], and CC5 and CC8, from *Cerastes cerastes* venom [26], also have a common subunit. Hence, sharing of subunits may represent an effective mechanism of structural and functional diversification of dimeric disintegrins.

It is worth noting that those disintegrins that block the function of $\alpha5\beta1$ integrin (EO4, VLO4, VB7 and VA6) contain RGD or KGD in both subunits, with the exception of EO4, which possesses a VGD sequence in its B subunit, and EMS11, which expresses an MLD motif in its A subunit (Figure 2, Table 2). The RGD motif is expressed at the apex of the integrin-binding loop of most monomeric disintegrins (Figure 3) and is responsible for the inhibitory activity of these disintegrins towards integrins that bind to ligands through RGD sites, including the fibronectin receptor, namely the $\alpha5\beta1$ integrin. Furthermore, the VGD sequence present in EC3A and also its related sequence MGD, found in EMF-10B, have been shown to contribute to the inhibitory activity of these disintegrins towards the $\alpha5\beta1$ integrin [6,7]. On the other hand, our results on $\alpha4\beta1$-inhibitory activities of EO5, EMS11 and VLO5 (Table 1) agree with previous studies showing that the specificity of EC3 for $\alpha4$ integrins resides in the MLD sequence of the B subunit [6].

The late discovery of dimeric disintegrins is because these are poor inhibitors of platelet aggregation, and monomeric disintegrins were first described as potent inhibitors of the platelet fibrinogen receptor, integrin αIIb$\beta3$ [4,33]. The isolation and characterization of disintegrins, which do not inhibit platelet aggregation (i.e. non-RGD-containing dimeric disintegrins), was achieved with the development, in the late 1990s, of cell adhesion inhibition assays using cell lines transfected with defined integrins [6,7,24]. Our results indicate that dimeric disintegrins are widely distributed in *Echis* and *Vipera* venoms, and probably also in the venoms of many other species of *Crotalidae* and *Viperidae*, which are rich sources of monomeric disintegrins. It is worth mentioning that non-RGD disintegrins are present in venoms which also contain RGD disintegrins [i.e. *E. ocellatus*: ocellatusin (RGD), EO4B (VGD), EO5 (MLD and VGD); *E. carinatus* (=*E.c. sochureki* or *E. sochureki*): echistatin (RGD), EC3 (VGD and MLD), EC6A (MLD); *V.l. obtusa*: VLO4 (RGD), obtustatin (KTS), VLO5 (VGD and MLD); *Eristocophis macmahoni*: eristostatin (RGD), EMF-10B (MGD)]. The large sequence and structural diversity exhibited by the different subfamilies of disintegrins (Figure 2) strongly suggests that disintegrins, like toxins from other venoms [34,35], have evolved rapidly by adaptative evolution driven by positive Darwinian selection. The co-existence in the same snake species of disintegrins with conserved RGD motif and disintegrins with variable non-RGD sequences supports the hypothesis [36] that, following gene duplication, one copy of the gene (i.e. the one coding for an RGD disintegrin) will divergently evolve under pressure dictated by the ancestral function (blocking of platelet aggregation), whereas the duplicate gene(s) (non-RGD disintegrin), unencumbered by a functional role, is (are) free to search for new physiological roles such as inhibition of non-RGD-dependent integrin receptors. As judged from the consensus sequences of the different disintegrin subfamilies shown in Figure 3, the integrin-binding loop represents a mutational 'hot spot' and the only conserved characteristic (except in obtustatin) is the presence of an acidic residue [D in short (dimeric)-, medium- and long-sized disintegrins; E or D in disintegrin/cysteine-rich domains] at the C-terminal site of the integrin-binding motif. The crystal structure of the extracellular segment of integrin $\alpha v\beta3$ in complex with an RGD ligand [37] shows that the peptide fits into a crevice between the αV propeller and the $\beta3$ A-domain. The arginine side chain is held in place by interactions with αV carboxylates 218 and 150, the glycine residue makes

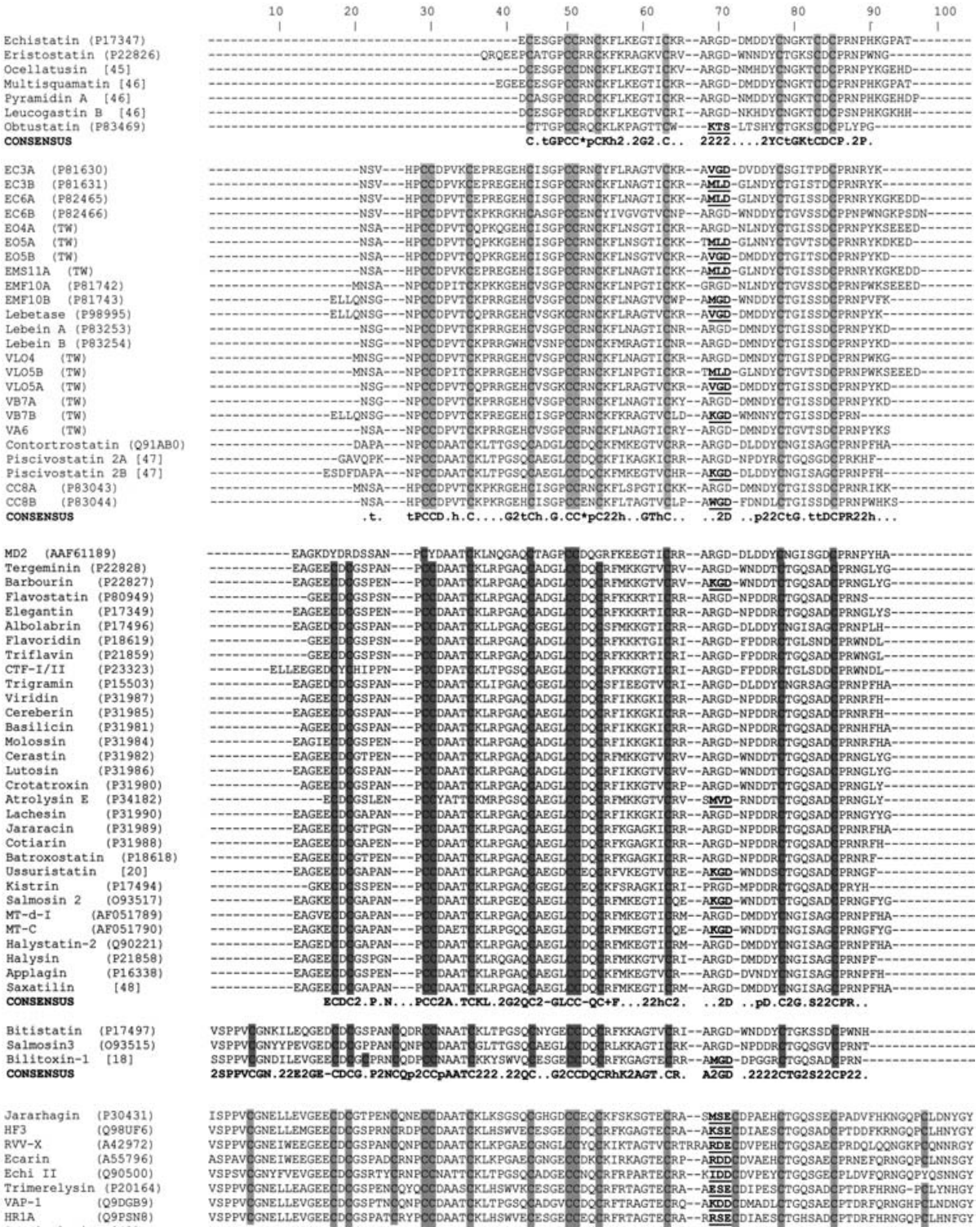

Figure 3 Figure legend see facing page

several hydrophobic interactions with αV and the aspartate ligand interacts primarily with βA residues. Thus, in agreement with our results, the conserved aspartate residue might be responsible for the binding of disintegrins to integrin receptors which share a β-subunit, whereas the other two residues of the integrin-binding motif (RG, MG, WG, ML, VG) may dictate the integrin specificity.

Phylogenetic analysis: structural diversification of disintegrins by disulphide bond engineering

Figure 4 displays a dendrogram for the multiple-sequence analysis of disintegrin domains listed in Figure 3, and it also includes the disintegrin domain of ADAMs from which snake venom disintegrins evolved after mammals and reptiles diverged [27]. The most prominent characteristic of this tree is that the members of the different subfamilies are almost perfectly clustered separately with their homologues, suggesting a possible evolutionary relationship between the different disintegrin subfamilies (Figure 5A). Proteins composed of disintegrin and cysteine-rich domains, derived from PIII snake venom metalloproteinases, are the closest homologues of cellular ADAMs. Comparison of full-length cDNA sequences of ADAMs and PIII SVMPs shows that the genes coding for the latter molecules possess 3′-untranslated regions, which include STOP codons after the cysteine-rich domain. Thus PIII SVMPs are not simply derived by proteolysis of ADAM molecules, but have rather evolved from a common ancestor after having lost the genetic information coding for protein regions downstream of the cysteine-rich domain (epidermal growth factor-like, transmembrane and cytoplasmic domains). Further deletions of gene regions coding for (i) the C-terminal portion of the disintegrin domain (including Cys-16) and the cysteine-rich domain and (ii) Cys-13, which is disulphide-bonded to Cys-16, gave rise to long-sized disintegrins (Figure 5A). Disintegrins are small in size and possess a high density of disulphide bonds. A close examination of the conserved cysteine residues in each disintegrin subfamily (Figure 3) strongly indicates that the structural diversity of disintegrins has been achieved during evolution through the selective loss of disulphide bonds (Figure 5A). Hence, mutations in the codon of Cys-1, along with a deletion of nine bases coding for the tripeptide CQ(D/N) from a long-sized disintegrin ancestor, resulted in the removal of the disulphide bond between Cys-1 and Cys-4 and the emergence of medium-sized disintegrins (Figure 5B). Further mutations involving the codons of the first two cysteine residues of medium-sized disintegrins (Cys-2 and Cys-3 in Figure 5B) yielded polypeptides with ten cysteine residues. The disulphide bond pattern of these disintegrin chains follows the same scheme as that of medium-sized disintegrins (Figure 5), except that the two cysteine residues (Cys-6 and Cys-7; Figure 5), which in medium-sized disintegrins are disulphide-bonded to Cys-3 and Cys-2 respectively, are engaged in two interchain disulphide bonds with homologous cysteine residues from another 10-cysteine-residue-containing disintegrin [17], giving rise to homo- and heterodimers [5–7,26,32,38,39]. The fact that the amino acid sequences of the subunits of the

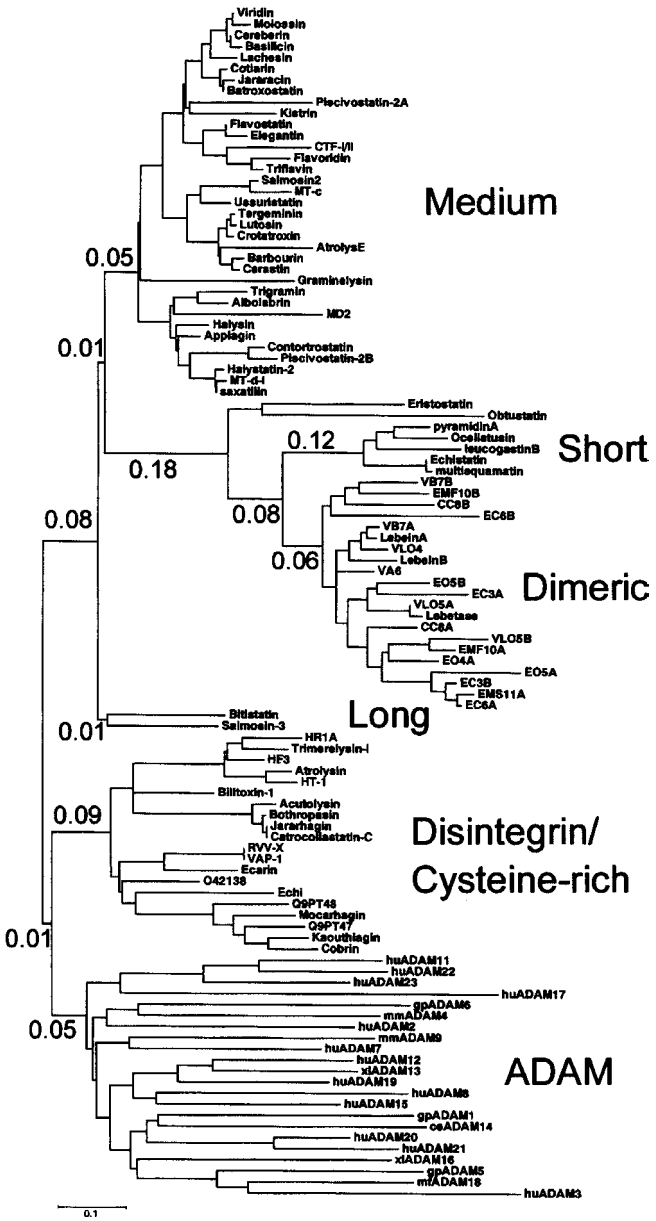

Figure 4 Dendrogram for the multiple-sequence analysis of disintegrin domains listed in Figure 3

The tree represents the minimum evolutionary distance estimated through neighbour joining using maximum likelihood distances. Maximum parsimony produced a similar topology. Representative disintegrin domains of human (hu), mouse (mm), guinea-pig (gp) and *Xenopus* (xl) ADAMs are also displayed. The length of the horizontal scale bar represents 10 % divergence. Phylogenetic distances at branch points are indicated.

dimeric disintegrins piscivostatin and contortrostatin cluster with the medium-sized disintegrins (Figure 4) further suggests that these dimeric disintegrins may have evolved from a medium-sized disintegrin ancestor. Finally, and although cDNA sequences

Figure 3 Multiple amino-acid sequence analysis of disintegrins

The one-letter code for amino acid nomenclature is used. Cysteine residues are shadowed in pale grey. Non-RGD integrin-binding tripeptide motifs are underlined and shown in bold. Amino acid characteristics which define the signature of each disintegrin subfamily are shown in the 'Consensus' line using the following code: a, aromatic (F, Y, W); h, hydrophobic (L, I, V, M, A); t, turn-like or polar (G, P, N, Q, H, S, T); −, negatively charged (E, D); +, positively charged (K, R); *, charged (E, D, K, R); p, conservative (N, D, Q, E); 2, one of the two residues in any sequence. Where available, databank accession numbers are given. TW, this work (present study). The amino acid sequences of the following disintegrins were extracted from primary references: ocellatusin [45], multisquamatin [46], pyramidin A [46], leucogastin B [46], piscivostatin 2A and 2B [47], ussuristatin [20], bilitoxin-1 [18], saxatilin [48] and graminelysin [49].

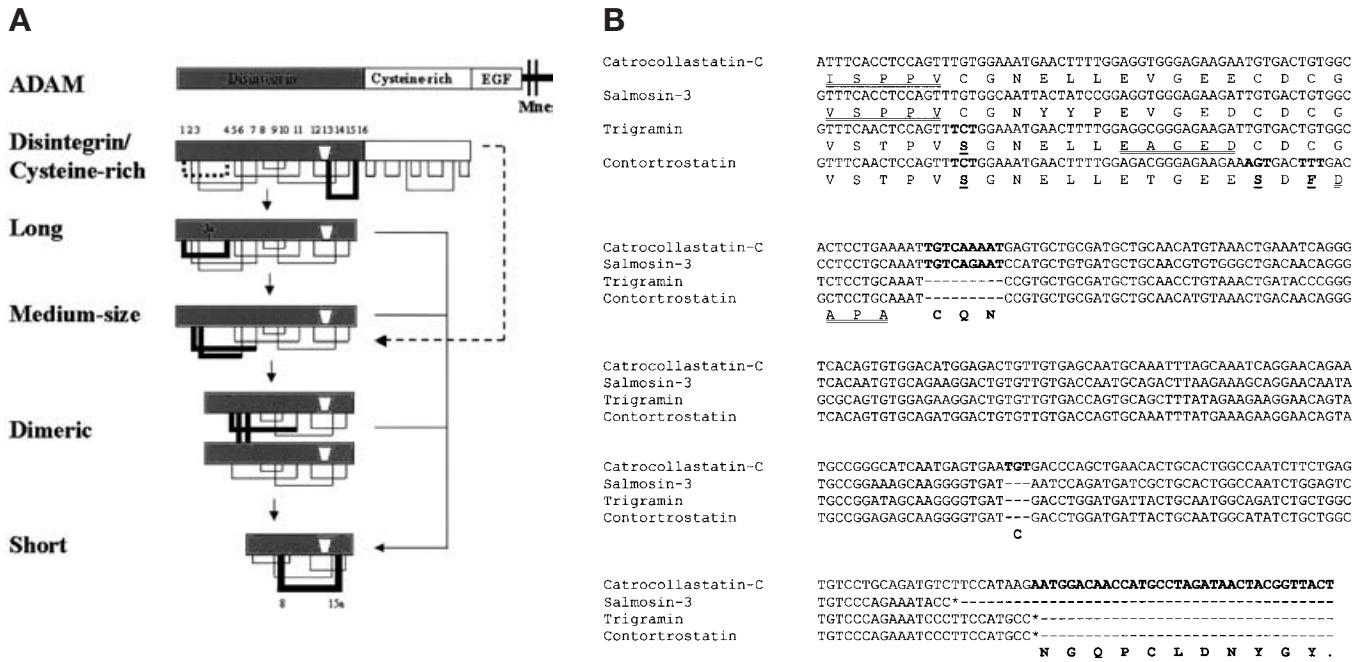

Figure 5 Proposed evolutionary relationship between the different disintegrin subfamilies

(**A**) Scheme of the domain organization and disulphide bond patterns of proteins from the different disintegrin subfamilies. A precursor ADAM molecule is shown at the top. Cysteine residues are numbered from 1 to 16. Disulphide bonds, which are removed in the hypothetical evolutionary pathway from disintegrin/cysteine-rich proteins to short-sized disintegrins, are indicated by thick lines, and possible evolutionary pathways in the evolution of the different disintegrin subfamilies are indicated by arrows. The disulphide bond Cys-1–4 absent from graminelysin, a member of the disintegrin/cysteine-rich subfamily, is indicated by a broken line. A hypothetical pathway from a gramelysin-type disintegrin to a medium-sized disintegrin is indicated by an arrow over the broken line. The cysteine residues engaged in the short-sized-disintegrin-specific disulphide bond are labelled. 3a indicates the position of an extra cysteine residue in bilitoxin-1. The position of the integrin-binding motif is shown as a white cone. (**B**) Alignment of the nucleotide sequences of cDNAs coding for representative members of the disintegrin subfamilies, catrocollastatin-C [41] (disintegrin/cysteine-rich), salmosin-3 [42] (long), trigramin [43] (medium-sized) and contortrostatin [44] (dimeric). Mutations and deletions affecting the cysteine residue content in the molecule are in boldface. N-terminal sequences of the mature proteins are double underlined.

of short-sized disintegrins are not available, the formation of short-sized disintegrins implies deletion or mutation of Cys-1–7 and the appearance of another cysteine residue between Cys-15 and Cys-16 (15a in Figure 5A), involved in the formation of a short-sized-disintegrin-specific disulphide bond with Cys-8, and which otherwise would remain unpaired. Clearly, genetic information is eagerly awaited to ascertain whether short-sized disintegrins have arisen from long/medium-sized or 10-cysteine-residue-containing disintegrins.

Although the vast majority of the disintegrins listed in Figure 3 might follow the canonical scheme outlined above, the evolutionary scenario of the disintegrin family might be more complex. Thus graminelysin departs from this pathway. It contains the Cys-13–16 disulphide bond specific to disintegrin/cysteine-rich domains, but clusters with the medium-sized disintegrins, and similar to them has serine in the place of Cys-1 and lacks the CQ(D/N) region. Hence, graminelysin might represent an intermediate step in an alternative route in the evolution of medium-sized disintegrins from disintegrin/cysteine-rich proteins. Bilitoxin-1, a long-sized disintegrin from *Agkistrodon bilineatus* venom [18], possesses an extra cysteine residue between Cys-3 and Cys-4 (Figure 3; also marked with an arrow in Figure 5A) involved in the formation of a disulphide-bonded homodimer. MD2, from *Agkistrodon acutus*, represents another unique disintegrin. It is closely related to medium-sized disintegrins, but lacks four cysteine residues (Cys-2, -3, -5 and -10), and its disulphide-bond pattern and aggregation state remain to be determined. Furthermore, proteins containing disintegrin and cysteine-rich domains have also been identified in the venoms of snakes belonging to the families *Atractaspidae* (mole vipers) and *Elapidae* (cobras, kraits, coral snakes) (kaouthiagin [40], atractaspin, mocarhagin, Q9PT47 and Q9PT48; Figure 3). Strikingly, two of these proteins, namely kaouthiagin from *Naja kaouthia* venom and Q9PT48 from *Atractaspis engaddensis* venom, have a large deletion including Cys-8, -9, -10 and -11 (Figure 3). Kaouthiagin expresses the HDCD motif in its disintegrin domain and an RGD sequence in its cysteine-rich domain, and has inhibitory activity on collagen-induced platelet aggregation with IC_{50} of 0.2 μM. Studies with synthetic peptides based on the HDCD and RGD motifs indicated that both sequences may act synergistically to block collagen-induced platelet aggregation [40]. On the other hand, the occurrence of disintegrins in venoms of neurotoxic snakes indicates that the distribution of disintegrins is not restricted to the haemorrhagic venoms of *Crotalidae* and *Viperidae* snakes.

The specificity of disintegrins is due to their disulphide-bonding framework and specific amino acids in intercysteine loops. The high content of disulphides plays a vital role in their stability and imposes a distinct protein folding, with a specific orientation of the loop regions. Our results support the view that the different disintegrin subfamilies have evolved from a common ADAM scaffold and that structural diversification occurred through disulphide bond engineering.

This work was financed by the Dirección General de Enseñanza Superior e Investigación Científica (Madrid, Spain) (grant no. BMC2001-3337; to J. J. C.) and the American Heart Association (Dallas, TX, U.S.A.; to C. M.).

REFERENCES

1 Markland, F. S. (1998) Snake venoms and the hemostatic system. Toxicon **36**, 1749–1800

2 Jia, L.-G., Shimokawa, K.-I., Bjarnason, J. B. and Fox, J. W. (1996) Snake venom metalloproteinases: structure, function and relationship to the ADAMs family of proteins. Toxicon **34**, 1269–1276

3 Kini, R. M. and Evans, H. J. (1992) Structural domains in venom proteins: evidence that metalloproteinases and nonenzymatic platelet aggregation inhibitors (disintegrins) from snake venoms are derived by proteolysis from a common precursor. Toxicon **30**, 265–293

4 McLane, M. A., Marcinkiewicz, C., Vijay-Kumar, S., Wierzbicka-Patynowski, I. and Niewiarowski, S. (1998) Viper venom disintegrins and related molecules. Proc. Soc. Exp. Biol. Med. **219**, 109–119

5 Trikha, M., De Clerk, Y. A. and Markland, F. S. (1994) Contortrostatin, a snake venom disintegrin, inhibits $\beta1$ integrin-mediated human metastatic melanoma cell adhesion and blocks experimental metastasis. Cancer Res. **54**, 4993–4998

6 Marcinkiewicz, C., Calvete, J. J., Marcinkiewicz, M. M., Raida, M., Vijay-Kumar, S., Huang, Z., Lobb, R. R. and Niewiarowski, S. (1999) EC3, a novel heterodimeric disintegrin from *Echis carinatus* venom, inhibits $\alpha4$ and $\alpha5$ integrins in an RGD-independent manner. J. Biol. Chem. **274**, 12468–12473

7 Marcinkiewicz, C., Calvete, J. J., Vijay-Kumar, S., Marcinkiewicz, M. M., Raida, M., Schick, P., Lobb, R. R. and Niewiarowski, S. (1999) Structural and functional characterization of EMF10, a heterodimeric disintegrin from *Eristocophis macmahoni* venom that selectively inhibits $\alpha5\beta1$ integrin. Biochemistry **38**, 13302–13309

8 Calvete, J. J., Wang, Y., Mann, K., Schäfer, W., Niewiarowski, S. and Stewart, G. J. (1992) The disulphide bridge pattern of snake venom disintegrins, flavoridin and echistatin. FEBS Lett. **309**, 316–320

9 Bauer, M., Sun, Y., Degenhardt, C. and Kozikowski, B. (1993) Assignment of all four disulphide bridges in echistatin. J. Protein Chem. **12**, 759–764

10 McLane, M. A., Vijay-Kumar, S., Marcinkiewicz, C., Calvete, J. J. and Niewiarowski, S. (1996) Importance of the structure of the RGD-containing loop in the disintegrins echistatin and eristostatin for recognition of αIIb$\beta3$ and αv$\beta3$ integrins. FEBS Lett. **391**, 139–143

11 Adler, M., Lazarus, R. A., Dennis, M. S. and Wagner, G. (1991) Solution structure of kistrin, a potent platelet aggregation inhibitor and GPIIb–IIIa antagonist. Science **253**, 445–448

12 Calvete, J. J., Schäfer, W., Soszka, T., Lu, W., Cook, J. J., Jameson, B. A. and Niewiarowski, S. (1991) Identification of the disulphide bond pattern in albolabrin, an RGD-containing peptide from the venom of *Trimeresurus albolabris*: significance for the expression of platelet aggregation inhibitory activity. Biochemistry **30**, 5225–5229

13 Klaus, W., Broger, C., Gerber, P. and Senn, H. (1993) Determination of the disulphide bonding pattern in proteins by local and global analysis of nuclear magnetic resonance data. Application to flavoridin. J. Mol. Biol. **232**, 897–906

14 Calvete, J. J., Schrader, M., Raida, M., McLane, M. A., Romero, A. and Niewiarowski, S. (1997) The disulphide bond pattern of bitistatin, a disintegrin isolated from the venom of the viper *Bitis arietans*. FEBS Lett. **416**, 197–202

15 Park, D., Kang, I., Kim, H., Chung, K., Kim, D.-S. and Yun, Y. (1998) Cloning and characterization of novel disintegrins from *Agkitrosdon halys* venom. Mol. Cell **8**, 578–584

16 Calvete, J. J., Moreno-Murciano, M. P., Sanz, L., Jürgens, M., Schrader, M., Raida, M., Benjamin, D. C. and Fox, J. W. (2000) The disulphide bond pattern of catrocollastatin C, a disintegrin-like/cysteine-rich protein isolated from *Crotalus atrox* venom. Protein Sci. **9**, 1365–1373

17 Calvete, J. J., Jürgens, M., Marcinkiewicz, C., Romero, A., Schrader, M. and Niewiarowski, S. (2000) Disulphide bond pattern and molecular modelling of the dimeric disintegrin EMF-10, a potent and selective integrin $\alpha_5\beta_1$ antagonist from *Eristocophis macmahoni* venom. Biochem. J. **345**, 573–581

18 Nikai, T., Taniguchi, K., Komori, Y., Masuda, K., Fox, J. W. and Sugihara, H. (2000) Primary structure and functional characterization of bilitoxin-1, a novel dimeric P-II snake venom metalloproteinase from *Agkistrodon bilineatus* venom. Arch. Biochem. Biophys. **378**, 6–15

19 Scarborough, R. M., Rose, J. W., Hsu, M. A., Phillips, D. R., Fried, V. A., Campbell, A. M., Nannizzi, L. and Charo, I. F. (1991) Barbourin. A GPIIb–IIIa-specific integrin antagonist from the venom of *Sistrurus M. barbouri*. J. Biol. Chem. **266**, 9359–9362

20 Oshikawa, K. and Terada, S. (1999) Ussuristatin 2, a novel KGD-bearing disintegrin from *Agkistrodon ussuriensis* venom. J. Biochem. (Tokyo) **125**, 31–35

21 Saudek, V., Atkinson, R. A. and Pelton, J. T. (1991) Three-dimensional structure of echistatin, the smallest active RGD protein. Biochemistry **30**, 7369–7372

22 Senn, H. and Klaus, W. (1993) The nuclear magnetic resonance solution structure of flavoridin, an antagonist of the platelet GPIIb–IIIa receptor. J. Mol. Biol. **232**, 907–925

23 Smith, K. J., Jaseja, M., Lu, X., Williams, J. A., Hyde, E. I. and Trayer, I. P. (1996) Three-dimensional structure of the RGD-containing snake toxin albolabrin in solution, based on ^{1}H NMR spectroscopy and simulated annealing calculations. Int. J. Pept. Protein Res. **48**, 220–228

24 Marcinkiewicz, C., Vijay-Kumar, S., McLane, M. A. and Niewiarowski, S. (1997) Significance of the RGD loop and C-terminal domain of echistatin for recognition of αIIb$\beta3$ and αv$\beta3$ integrins and expression of ligand-induced binding sites. Blood **90**, 1565–1575

25 Shimokawa, K.-I., Jia, L.-G., Shannon, J. D. and Fox, J. W. (1998) Isolation, sequence analysis, and biological activity of atrolysin E/D, the non-RGD disintegrin domain from *Crotalus atrox* venom. Arch. Biochem. Biophys. **354**, 239–246

26 Calvete, J. J., Fox, J. W., Agelan, A., Niewiarowski, S. and Marcinkiewicz, C. (2002) The presence of the WGD motif in CC8 heterodimeric disintegrin increases its inhibitory effect on $\alpha_{IIb}\beta_3$, $\alpha_v\beta_3$, and $\alpha_5\beta_1$ integrins. Biochemistry **41**, 2014–2021

27 Moura-Da-Silva, A. M., Theakston, R. D. G. and Crampton, J. M. (1996) Evolution of disintegrin cysteine-rich and mammalian matrix-degrading metalloproteinases: gene duplication and divergence of a common ancestor rather than convergent evolution. J. Mol. Evol. **43**, 263–269

28 Altschul, S. F., Madden, T. L., Schäffer, A. A., Zhang, J., Zhang, Z., Miller, W. and Lipman, D. J. (1997) Gapped BLAST and PSI-BLAST: a new generation of protein database search programs. Nucleic Acids Res. **25**, 3389–3402

29 Thompson, J. D., Higgins, D. J. and Gibson, T. J. (1994) CLUSTAL W: the sensitivity of progressive multiple sequence alignment through sequence weighting, position-specific gap penalties and weight matrix choice. Nucleic Acids Res. **22**, 4673–4680

30 Felsenstein, J. (1995) PHYLIP (Phylogeny Interface Package) version 3.57c, Department of Genetics, University of Washington, Seattle, WA

31 Kumar, S., Tamura, K., Jakobsen, I. B. and Nei, M. (2001) Mega2: Molecular Evolutionary Genetics Analysis software. Bioinformatics **17**, 1244–1245

32 Marcinkiewicz, C., Taooka, Y., Yokosaki, Y., Calvete, J. J., Marcinkiewicz, M. M., Lobb, R. R., Niewiarowski, S. and Sheppard, D. (2000) Inhibitory effects of MLDG-containing heterodimeric disintegrins reveal distinct structural requirements for interaction of the integrin $\alpha9\beta1$ with VCAM-1, tenascin-C, and osteopontin. J. Biol. Chem. **275**, 31930–31937

33 Huang, T.-F., Holt, J. C., Lukasiewicz, H. and Niewiarowski, S. (1987) Trigramin. A low molecular weight peptide inhibiting fibrinogen interaction with platelet receptors expressed on glycoprotein IIb–IIIa complex. J. Biol. Chem. **262**, 16157–16163

34 Duda, Jr, T. F. and Palumbi, S. R. (1999) Developmental shifts and species selection in gastropods. Proc. Natl. Acad. Sci. U.S.A. **96**, 6820–6823

35 Kordis, D., Krizaj, I. and Gubensek, F. (2002) Functional diversification of animal toxins by adaptative evolution. In Perspectives in Molecular Toxinology (Ménez, A., ed.), pp. 401–419, John Wiley & Sons, New York

36 Trabesinger-Ruef, N., Jermann, T., Zankel, T., Durrant, B., Frank, G. and Benner, S. A. (1996) Pseudogenes in ribonuclease evolution: a source of new biomolecular function? FEBS Lett. **382**, 319–322

37 Xiong, J.-P., Stehle, T., Zhang, R., Joachimiak, A., Frech, M., Goodman, S. L. and Arnaout, M. A. (2002) The crystal structure of the extracellular segment of integrin αv$\beta3$ in complex with an Arg-Gly-Asp ligand. Science **296**, 151–155

38 Gasmi, A., Srairi, N., Guermazi, S., Dkhil, H., Karoui, H. and El Ayeb, M. (2001) Amino acid structure and characterization of a heterodimeric disintegrin from *Vipera lebetina* venom. Biochim. Biophys. Acta **1547**, 51–56

39 Zhou, Q., Hu, P., Ritter, M. R., Swenson, S. D., Argounova, S., Epstein, A. L. and Markland, F. S. (2000) Molecular cloning and functional expression of contortrostatin, a homodimeric disintegrin from southern copperhead snake venom. Arch. Biochem. Biophys. **375**, 278–288

40 Ito, M., Hamako, J., Sakurai, Y., Matsumoto, M., Fujimura, Y., Suzuki, M., Hashimoto, K., Titani, K. and Matsui, T. (2001) Complete amino acid sequence of kaouthiagin, a novel cobra venom metalloproteinase with two disintegrin-like sequences. Biochemistry **40**, 4503–4511

41 Shimokawa, K.-I., Shannon, J. D., Jia, L.-G. and Fox, J. W. (1997) Sequence and biological activity of catrocollastatin-C: a disintegrin-like/cysteine-rich two domain protein from *Crotalus atrox* venom. Arch. Biochem. Biophys. **343**, 35–43

42 Neeper, M. P. and Jacobson, M. A. (1990) Sequence of a cDNA encoding the platelet aggregation inhibitor trigramin. Nucleic Acids Res. **18**, 4255

43 Park, D. S., Kang, I., Kim, H., Chung, K., Kim, D. S. and Yun, Y. D. (1998) Cloning and characterization of novel disintegrins from *Agkistrodon halys* venom. Mol. Cell **8**, 578–584

44 Zhou, Q., Smith, J. B. and Grossman, M. H. (1995) Molecular cloning and expression of catrocollastatin, a snake-venom protein from *Crotalus atrox* (western diamondback rattlesnake) which inhibits platelet adhesion to collagen. Biochem. J. **307**, 411–417
45 Smith, J. B., Theakston, R. D. G., Coelho, A. L. J., Barja-Fidalgo, C., Calvete, J. J. and Marcinkiewicz, C. (2002) Characterization of a monomeric disintegrin, ocellatusin, present in the venom of the Nigerian carpet viper, *Echis ocellatus*. FEBS Lett. **512**, 111–115
46 Okuda, D., Nozaki, C., Sekiya, F. and Morita, T. (2001) Comparative biochemistry of disintegrins isolated from snake venom: consideration of the taxonomy and geographical distribution of snakes in the genus *Echis*. J. Biochem. (Tokyo) **129**, 615–620
47 Okuda, D. and Morita, T. (2001) Purification and characterization of a new RGD/KGD-containing dimeric disintegrin, Piscivostatin, from the venom of *Agkistrodon piscivorus piscivorus*: the unique effect of Piscivostatin on platelet aggregation. J. Biochem. (Tokyo) **130**, 407–415
48 Hong, S.-Y., Koh, Y.-S., Chung, K.-H. and Kim, D.-S. (2002) Snake venom disintegrin, saxatilin, inhibits platelet aggregation, human umbilical vein endothelial cell proliferation, and smooth muscle cell migration. Thrombosis Res. **105**, 79–86
49 Wu, W. B., Chang, S. C., Liau, M. Y. and Huang, T. F. (2001) Purification, molecular cloning and mechanism of action of graminelysin I, a snake-venom-derived metalloproteinase that induces apoptosis of human endothelial cells. Biochem. J. **357**, 719–728

Received 6 November 2002/11 March 2003; accepted 1 April 2003
Published as BJ Immediate Publication 1 April 2003, DOI 10.1042/BJ20021739